The effects of local lattice distortion in non-isochoric alloys: CuPd and CuBe

1996 J. Phys.: Condens. Matter 8 2915

(http://iopscience.iop.org/0953-8984/8/17/005)

J. Phys.: Condens. Matter **8** (1996) 2915–2927. Printed in the UK

The effects of local lattice distortion in non-isochoric alloys: CuPd and CuBe

Tanusri Saha and Abhijit Mookerjee
International Centre for Theoretical Physics, Trieste, Italy†

Received 28 July 1995, in final form 4 December 1995

Abstract. We study here the effect of local lattice distortion on the electronic structure of non-isochoric alloys with large size difference between the constituents using the augmented space recursion. In particular we study such effects in CuPd and CuBe alloys.

1. Introduction

In a series of recent communications the authors and coworkers have proposed the augmented space recursion (ASR) in conjunction with the tight-binding linearized muffin tin orbitals method (TB LMTO) of Andersen and coworkers as a generalized and efficient method for dealing with the electronic structure of disordered alloys [1]. One of the advantages of the method is that it can take into account inhomogeneous disorder, such as effects of clustering [1], short-ranged ordering effects [2] and inhomogeneous concentration profiles due to segregation at surfaces [3]. In this communication we study another important source of local inhomogeneities, namely that caused by local lattice distortions which necessarily arise when atoms with very different sizes are alloyed together.

Describing the random alloy Hamiltonian by a tight-binding-like scheme, disorder can be in the on-site atomic levels as well as in the off-diagonal transfer terms. In some alloys there is a strong randomness both in the atomic levels and in the transfer integrals. It has been shown [4] that for such alloys the constituents come from different rows of the periodic table. As a result there exists an appreciable mismatch between atomic radii of the constituents. This non-isochoricity in turn results in local distortion of the underlying lattice. In the usual treatments of alloys with substitutional disorder, all atoms are placed on a regular lattice whose lattice spacing is obtained either by assuming Vegard's law or by energy minimization with respect to the lattice constant. Though such an approach gives reasonable results for those alloys made out of components with nearly equal atomic radii, it overlooks the differential expansion (contraction) around larger (smaller) atom for alloys with components of different sizes. This local distortion of the ideal lattice has been verified by extended x-ray absorption fine-structure experiments [5]. It has also been suggested [6] that neglect of such effects in the charge self-consistent Korringa–Kohn–Rostoker coherent potential approximation (KKR CPA) [7] has led to disagreement between predicted features of KKR CPA electronic density of states of non-isochoric alloys with that of experiments.

† Permanent address: S N Bose National Centre for Basic Sciences, J D Block, Sector 3, Calcutta 700091, India.

0953-8984/96/172915+13$19.50

Such non-isochoric alloys with their associated relaxation effects are important for a number of purposes. Various phenomenological theories of alloying, such as Hume–Rothery rules, state that size effects are significant with regard to phase stability. The problem of size effect in the context of the Li–Al phase diagram has been considered approximately by Sluiter *et al* [8]. Another effect is the influence of relaxation on the local magnetic moments of dilute alloys [9].

Calculation for a large-atom impurity in host atoms of smaller size has been carried out within the KKR–Green function method [10]. An attempt to study the influence of lattice relaxation on electronic structure of concentrated alloys has been made by Kudrnovský and Drchal [11] within the linearized muffin tin orbitals coherent potential approximation (LMTO CPA) framework. Since lattice relaxation introduces a kind of positional disorder, in addition to disorder in scattering properties of potentials, it essentially brings about disorder in the structure matrix describing the geometry of the lattice, leading to a complicated off-diagonal disorder. The CPA, which treats only the site-diagonal disorder, cannot be applied to such random Hamiltonian without further simplifying assumptions. Kudrnovský and Drchal [11] have suggested as approximate way of treating this through a mapping of the Hamiltonian (via the assumption of a multiplicative form of the off-diagonal term) onto an effective Hamiltonian with diagonal disorder *alone*. Such a mapping involves approximation of the disorder in the structure factor by the unrelaxed structure matrix between two sites multiplied by a random factor which depends on the occupancy of the sites.

In the ASR formalism, the form of the Hamiltonian is kept intact with both diagonal and off-diagonal disorder so that the disorder in structure factor arising out of lattice distortion can be dealt with ease. We wish to present this methodology as a formally exact way of dealing with off-diagonal disorder. There will be no need to assume a multiplicative form of the off-diagonal terms of the Hamiltonian. Structural disorder arising out of size mismatch is one candidate where a simple multiplicative form of an effective Hamiltonian may no longer be valid. It is worth mentioning that recently [12] there has been a study of the relaxation effect in Cu-rich Pd alloy where application of the linear augmented plane wave (LAPW) band structure technique has been made to repeated super-cells with constructed quasi-random structures to simulate the relaxed lattice structure. Such super-cell calculations with large numbers of atoms per unit cell may be found to be computationally heavy and may be used as a yardstick against which to compare the numerical results of our computationally less expensive technique.

Two representative systems of non-isochoric alloys with associated lattice distortion are CuPd alloys and CuBe alloys. In the former case for Cu-rich alloys the lattice gets locally expanded with the introduction of large Pd atoms into the matrix of small Cu atoms and in the latter case distortion in the Cu-rich regime arises due to local contraction when small Be atoms sit in a matrix of large Cu atoms. It may be noted that the beryl bronzes (CuBe alloys with small concentrations of Be) are extremely resistant to plastic deformations. It has long been suggested that this is due to the pinning of the motion of extended defects during plastic deformation by the local lattice distortions at the Be sites. In section 2.1 we give a short summary of the TB LMTO formalism along with ASR. Section 2.2 deals with ASR in the presence of positional disorder. In section 3 we present computational details with a stress on multi-spin coding technique and use of point group symmetry in augmented space which makes the implementation of ASR feasible. Section 4 has been devoted to results and discussion where application of the developed formalism has been made to CuPd and CuBe alloys.

2. Methodology

2.1. The augmented space recursion

The LMTO method for self-consistent calculations of electronic structures of solids was introduced by Andersen and Jepsen [13]. It has been described in great detail in a recent monograph [14]. We shall indicate here only those points which are of specific importance for the present work. We stress here that the transformation of the canonical LMTO into a first-principles tight-binding method with a sparse Hamiltonian representation is *essential* for an effective use of the recursion technique which is the basis of our methodology.

In LMTO representation within atomic sphere approximation, the basis functions have the form

$$\chi^{\alpha}_{RL}(r_R) = \phi_{RL}(r_R) + \sum \dot{\phi}^{\alpha}_{R'L'}(rR)h^{\alpha}_{RL,R'L'}$$

where ϕ is the product of a spherical harmonic and the solution $\phi_{\nu RL}(|r_R|)$ of the radial wave equation inside the sphere centred at R for a certain energy $E_{\nu RL}$, which is in principle arbitrary, but in the energy range of interest. The functions $\dot{\phi}^{\alpha}$ are linear combinations of the products ϕ and their energy derivatives $\dot{\phi}$. The actual choice of how this linear combination is made determines the basis. The matrix h is given by

$$h^{\alpha} = C^{\alpha} - E_{\nu} + (\Delta^{\alpha})^{1/2} S^{\alpha} (\Delta^{\alpha})^{1/2}$$

where C^{α} and Δ^{α} are the diagonal *potential parameter matrices*. They depend on the potentials inside the atomic spheres, the representation (α) chosen and on the atomic sphere radii. The S matrix is a structure matrix which depends only on the representation (α) and on the geometrical arrangement of the atomic sites. In terms of the canonical structure matrix S^0, S^{α} is given by

$$S^{\alpha} = S^0(1 - \alpha S^{\alpha})^{-1}$$

where α denotes a diagonal matrix, specifying the representation.

In recursion calculations it is practical to work with an orthonormal sparse representation. For this purpose it is advantageous to work in the γ representation. It must be noted, however, that the structure matrix in the γ representation is itself random in an intrinsic way. It is useful therefore to rewrite the Hamiltonian in terms of that in the most localized (or β) representation. The Hamiltonian in the γ representation, which is correct up to second order in $(E - E_{\nu})$, is given by

$$H^2 = E_{\nu} + h^{\gamma}. \tag{1}$$

The overlap matrix in this representation is a unit, diagonal matrix and therefore it fulfills the orthogonality condition required for recursion purposes. Expansion of h^{γ} in terms of the most localized short-ranged h_{α} is given by

$$h^{\gamma} = h^{\alpha} - h^{\alpha} o h^{\alpha} - \cdots \tag{2}$$

where the matrix o is diagonal in RL representation and its value is determined by the logarithmic derivative of the function ϕ at the sphere boundary. For a particular choice of $\alpha = \beta$ which are independent of crystal structure given by

$$\beta = \begin{cases} 0.3485 & l = 0 \\ 0.0530 & l = 1 \\ 0.0107 & l = 2 \end{cases}$$

the screened structure constant S^β becomes particularly short ranged with a universal exponential decay for different structures (fcc, bcc, hcp, etc). Due to the exponential behaviour of the structure factor, even for s and p bands it is not necessary to consider interactions beyond second-nearest neighbours.

If the power series given by (2) is truncated after the first-order term, we obtain a two-centre *sparse* Hamiltonian. This Hamiltonian is correct up to first order in $(E - E_\nu)$ and it has been shown that it gives satisfactory band structure description for most solids except those with very broad bands [15]. However, since each term in the second and subsequent terms in the expansion are themselves two-centred and *sparse*, their inclusion in the recursion method introduces no difficulty. In subsequent sections we will use the first-order, tight-binding two-centre form of the LMTO Hamiltonian given by

$$H^1 = C^\beta + (\Delta^\beta)^{1/2} S^\beta (\Delta^\beta)^{1/2}.$$

Again, both the augmented space formalism and the recursion method have been described in great detail in earlier work [14, 17]. We shall only emphasize those points here which are of relevance to the present work and refer the reader to the articles referenced above for the details.

In the augmented space formalism, we construct a non-random Hamiltonian defined on a new enlarged Hilbert space, which is a direct product of the Hilbert space spanned by the original Hamiltonian basis set and the configuration space which is spanned by the various allowed configuration states of the disordered Hamiltonian. The augmented space theorem [18] then relates the configuration averaging to projection onto a particular subspace: the so-called *sum space* [19, 20]. This configuration averaging in the augmented space is *exact* and does not involve any single-site approximation as in CPA and treats both diagonal and off-diagonal disorder on an equal footing.

The whole process can be summarized in the following basic steps.

(i) Since the probability density $p_i(n_i)$ of a random variable n_i associated with the Hamiltonian is a positive semi-definite function and if we assume all its moments to be finite, we may find a self-adjoint operator $M^{(i)}$ in a configuration space $\phi^{(i)}$ such that $p_i(n_i)$ can be expressed as its spectral density

$$p_i(n_i) = -1/\pi \, \mathrm{Im}(\langle \nu_0^i | (n_i - M^{(i)})^{-1} | \nu_0^i \rangle).$$

This is the inverse of the well known problem of obtaining a local density of states starting from a self-adjoint Hamiltonian H. If $p_i(n_i)$ can be expressed in continued fraction expansion, then the representation of $M^{(i)}$ is a tri-diagonal matrix with continued fraction coefficients in diagonal and off-diagonal positions.

(ii) The averaged quantity $\int f(n_i) p_i(n_i)$ can be shown to be given by the matrix element $\langle \nu_0^i | \tilde{f}(M^{(i)}) | \nu_0^i \rangle$ where $\tilde{f}$ is the same functional of $M^{(i)}$ as f was of n_i.

(iii) For more than one random variable we define a product of space $\Phi = \prod^{\otimes} \phi^{(i)}$. This is spanned by states in which the set of variables n_i assumes one of its configurations. The averaged quantity $\langle f \rangle$ is now given by $\langle \nu_0 | \tilde{f}(M^{(i)}) | \nu_0 \rangle$ where $|\nu_0\rangle = \prod^{\otimes} |\nu_0\rangle^i$ spans the so-called sum space, which is a subspace of Φ. A little algebra will show us that $|\nu_0\rangle = \prod_i^{\otimes} (\sum_{\lambda i} \sqrt{p_{\lambda i}} |\lambda_i\rangle)$ where $|\lambda_i\rangle$ are the eigenstates of $\tilde{M}^{(i)}$ and $\{p_{\lambda i}\}$ are the associated probability weights.

The calculation of $\langle f \rangle$ thus reduces to calculating a particular matrix element in the augmented space. For electronic structure calculations in a disordered system, f is chosen to the the Green function $(zI - H(\{n_i\}))^{-1}$ where H is the Hamiltonian of the system and n_i are the random site occupation variables.

An efficient algorithm for calculating diagonal matrix elements of the resolvent or the Green function is provided by the recursion method introduced by Haydock and coworkers [16]. Given the starting vector $|\psi_0\rangle = |i, \nu_0\rangle$ in augmented space one generates a discrete chain of vectors $|\psi_i\rangle$ through the following set of operations:

$$\tilde{H}|\psi_i\rangle = a_i|\psi_i\rangle + b_{i+1}|\psi_{i+1}\rangle + b_i|\psi_{i-1}\rangle$$
$$b_0^2 = \langle\psi_0|\psi_0\rangle$$
$$b_i^2 = \langle\psi_i|\tilde{H}|\psi_{i+1}\rangle$$
$$a_i = \langle\psi_i|\tilde{H}|\psi_i\rangle$$

where $\tilde{H}$ is the operator defined in the full augmented space which is constructed by substituting the random site occupation variables $\{n_i\}$ by their associated self-adjoint operator $\{M^{(i)}\}$.

This prescription essentially transforms the effective Hamiltonian H to a trigonal form and thus leads directly to a continued fraction representation for the averaged Green function matrix element $\langle\psi_0|G|\psi_0\rangle = [G_{ii}]_{av}$. If the algorithm is stopped after L steps, L exact levels of the continued fraction are obtained. The recursion algorithm after L steps contains a contribution only from the central cluster containing $O(L^3)$ sites in the augmented space. For eliminating such a finite-cluster effect L steps of recursion coefficients are appended with a terminator which mimics the asymptotic part of the continued fraction.

2.2. ASR with structural disorder

The discussion of the previous section reveals that determination of the configuration averaged Green function in augmented space formalism amounts to determination of the diagonal matrix element of the resolvent associated with the effective Hamiltonian $\tilde{H}$ defined on the expanded augmented space, formed by replacing the random site variables n_i by self-adjoint operators $\tilde{M}^{(i)}$. The random Hamiltonian for a binary AB alloy described under the framework of the tight-binding LMTO basis is given by

$$H^{\beta} = \sum_i \sum_j \sum_L \sum_{L'} H^{\beta}_{iL,jL'} \mathcal{T}_{ij} \otimes \mathcal{T}_{LL'} \tag{3}$$

where

$$\begin{aligned} H^{\beta}_{iL,jL'} = {} & \sum \{C_L^A n_i + C_L^B (1 - n_i)\} \delta_{ij} \delta_{LL'} \\ & + \sum \sum \{(\Delta^{(A)})_L^{1/2} n_i + (\Delta^B)_L^{1/2} (1 - n_i)\} \\ & \times S^{\beta}_{iL,jL'} \{(\Delta^A)_{L'}^{1/2} n_j + (\Delta^B)_{L'}^{1/2} (1 - n_j)\} \end{aligned} \tag{4}$$

and $\mathcal{T}_{ij}$ is the projection operator $|i\rangle\langle i|$ if $i = j$ and the transfer operator $|i\rangle\langle j|$ if $i \neq j$. The potential parameters C_L and Δ_L at the sites i can be of A type or B type depending upon whether n_i is 0 or 1 (i.e. whether the site i is occupied by an A atom or a B atom).

In the absence of any positional disorder, the structure matrix in the most localized (β) representation which characterizes the underlying lattice structure is non-random. However, for non-isochoric alloys, the minority component introduced in the matrix of the majority component is shifted from the unrelaxed lattice positions. In other words where such a minority components sits the lattice locally deviates from that of a regular lattice.

The effect of lattice distortion depends on the immediate environment as the structure matrix essentially vanishes beyond the second-nearest neighbour for most of the closed

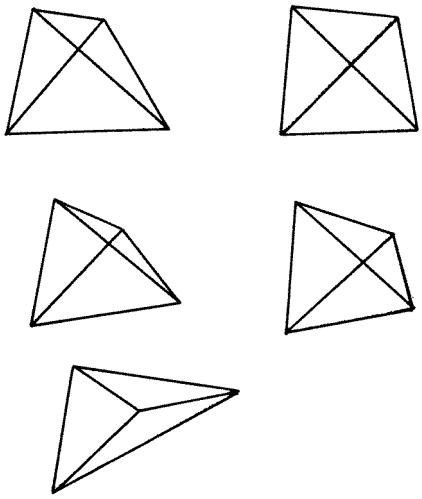

Figure 1. Structure of a tetrahedron fcc cluster for various possible occupations of vertices by A and B atoms.

structures. As an example, on a fcc lattice we can identify the smallest tetrahedral units of nearest-neighbour atoms. Possible combinations of A and B atoms occupying the corners of the units can be of the types AAAA, AAAB, AABB, ABBB and BBBB shown in figure 1. The configurations obtained by rotation from another configuration have some contribution to the structure matrix. Thus the structure matrix element between two points occurring in the unit will be given by

$$\begin{aligned} S^{\beta}_{iL,jL'} = {} & S^{\beta(AAAA)}_{iL,jL'} n_i n_j n_k n_m + S^{\beta(AAAB)}_{iL,jL'} [n_i n_j n_k (1-n_m) + (1-n_i) n_j n_k n_m + \cdots \\ & + n_i (1-n_j) n_k n_m + n_i n_j (1-n_k) n_m] + \cdots \\ & + S^{\beta(AABB)}_{iL,jL'} [n_i n_j (1-n_k)(1-n_m) + (1-n_i) n_j (1-n_k) n_m + \cdots \\ & + (1-n_i)(1-n_j) n_k n_m + (1-n_i) n_j n_k (1-n_m) + \cdots \\ & + n_i (1-n_j)(1-n_k) n_m + n_i (1-n_j) n_k (1-n_m)] + \cdots \\ & + S^{\beta(BBBA)}_{iL,jL'} [n_i (1-n_j)(1-n_k)(1-n_m) + (1-n_i) n_j (1-n_k)(1-n_m) + \cdots \\ & + (1-n_i)(1-n_j) n_k (1-n_m) + (1-n_i)(1-n_j)(1-n_k) n_m] + \cdots \\ & + S^{\beta(BBBB)}_{iL,jL'} (1-n_i)(1-n_j)(1-n_k)(1-n_m) \end{aligned} \tag{5}$$

where n_k and n_m describe the influence of the local environment on the structure matrix element connecting points i and j. This description takes into account both the effect of distortions of the distance bewteen i and j and the angular distortion of the square as we go from one configuration to another.

For the fcc lattice with structure matrix practically vanishing beyond the first-nearest-neighbour shell, the number of such inequivalent configurations will be 144. Consideration of all these configurations will lead to an exact treatment of the distortion effect up to the first-nearest-neighbour environment. However since the computational effort very quickly become prohibitive with the numerous possible values assumed by the S matrix, we will assume that the influence of other nearest neighbours on the structure matrix element connecting each atom with a particular neighbour to be small. *This is the terminal point*

approximation [24]. In this approximation the principal distortion taken into account is the *bond stretching/contraction* and all terms involving n_k and n_m in the example of plaquettes are replaced by the averages so that the effect of angular distortions is only taken in an average sense. Invoking the terminal point approximation the number of inequivalent configurations becomes three.

$$S^{\beta}_{iL,jL'} = S^{\beta(AA)}_{iL,jL'} n_i n_j + S^{\beta(AB)}_{iL,jL'}[n_i(1-n_j) + n_j(1-n_i)] + S^{\beta(BB)}_{iL,jL'}(1-n_i)(1-n_j). \tag{6}$$

The structural model used in our calculation is as follows. In the case without lattice relaxation the Wigner–Seitz radii of both the A and the B components are the same (say, a). On the other hand, for the case with lattice distortion, the Wigner–Seitz radius of the *larger* atom is taken to be $a(1+r)$, where r measures the degree of lattice distortion. The degree of lattice distortion used in our calculation is based on the rigid ion structure model (RIS) [21]. According to this model the lattice relaxes in such a way as to keep all the nearest-neighbour interatomic distances close to the sum of corresponding atomic radii. For CuPd alloys this model slightly overestimates the degree of lattice relaxation. In the low-concentration limit, the outward shift of Pd atoms is around 3.5% according to RIS, while EXAFS experiments indicate around 2%.

Let us take as an example the calculation of S^{AB}. This matrix connects an A atom at the site (000) and a B atom, which in the undistorted case should have been at the position (110) is now at $(1+d, 1+d, d)$. We have assumed that the lattice expands equally in the x, y and z directions. With these new coordinates and assuming that all other neighbouring coordinates are fixed at undistorted fcc positions (which is the essence of the terminal point approximation), we solve the Dyson equation to get S^{AB}. This takes into account both the effect of radial distortion (the nearest-neighbour distance is now $\sqrt{(2+4d+3d^2)}$ instead of $\sqrt{2}$) as well as angular distortion (the nearest-neighbour vector is $(1+d, 1+d, d)$ instead of (110)).

CPA calculations involve a single-site approximation and cannot deal with off-diagonal disorder with tri-modal probability distribution. One has to make further approximations at this point. Augmented space recursion, being free from such limitations, can deal with this off-diagonal disorder exactly. The effective Hamiltonian in the augmented space is then constructed by replacing the site occupation variable n_i by operator M_i defined in the configuration space. An examination of the Hamiltonian in augmented space reveals that it involves four possible terms, a term describing the uniform background against which the fluctuations are measured, a term describing fluctuation at the site i, a term describing fluctuation at the site j, a neighbouring site of i, and finally a term describing joint fluctuations at both the sites i and j.

For binary probability distributions the matrix M_i is given by

$$M_i = x\mathcal{P}^i_0 + (1-x)\mathcal{P}^i_1 + \sqrt{x(1-x)}(\mathcal{T}_{01} + \mathcal{T}_{10})$$

where $\mathcal{P}^i_0$ and $\mathcal{P}^i_1$ are the projection operators corresponding to states 0 and 1 respectively and $\mathcal{T}^i_{01}$ and $\mathcal{T}^i_{10}$ are the transfer operators between states characterized by 0 and 1 at the site i. Once the Hamiltonian and its operations are defined in augmented space it is now a trivial task to apply the recursion method to obtain the continued fraction coefficients of the configuration averaged Green function. The degree of lattice distortion is however a delicate problem which calls for the first-principles treatment including minimization of the total energy. The corresponding calculations should provide both displacement of atoms and the electronic structure in the relaxed lattice. For example, a structural determination is possible using a semi-empirical molecular dynamics and the resulting relaxed structure

could be used for a final first-principles electronic structure calculation. As far as we are aware, a full-scale first-principles molecular dynamics of transition metals is still not widely available. For our comparison with parallel works, we have chosen distortions consistent with those used for super-cell calculations.

3. Computational details

The densities of states have been found by the recursion method with the augmented space Hamiltonian. The augmented space map is generated from a real space cluster of 400 atoms. We have generated a sequence of eight couples of continued fraction coefficients for s, p and d states and the terminating scheme of Lucini and Nex [22] has been used. Regarding the issue of charge self-consistency we have followed the approximate yet accurate and consistent scheme of charge self-consistency proposed by Andersen *et al* [23]. Here the charge neutrality is achieved by exploiting the flexibility in the choice of sizes of Wigner–Seitz spheres of constituents in binary alloys. It involves scaling of the atomic sphere radii of alloy species with the aid of a volume derivative correction in such a way that the spheres are approximately charge neutral, a fact discussed in great detail by Kudrnovský and Drchal [24]. Though the augmented space formalism has been recognized as a powerful tool for configuration averaging, its implementation so far has been restricted to model systems. This was because standard recursion cannot deal with the large rank of the augmented space. In particular, the nearest-neighbour map which has to be initially stored for any recursion is too large for storage and manipulations on this map are time consuming. We have reduced this problem to a tractable one by an explicit use of bit manipulation techniques and reduction of the large augmented space to a manageable irreducible subspace on which the recursion could be carried out. As these points have already been described in detail elsewhere [25] we will only mention the salient points. The basis vectors defined in the configuration space, carrying information about the occupation variable at each site, are strings of zeros and ones. This allows us to extensively borrow the Ising computational methodology [26] which involves storage of configuration states in binary words and use of logical operations to describe the action of the augmented space Hamiltonian. The binary word representation of configuration states leads to large-scale saving of disk space while the use of logical operations makes the computation faster. The work-load of augmented space recursion is further reduced by exploiting the symmetry of the Hamiltonian. The symmetry of the Hamiltonian arises from that of the underlying lattice and from homogeneity of disorder. It has been shown by Gallagher [27] that if the starting state of recursion belongs to the irreducible representation of the Hamiltonian then the states generated in the process of recursion belong to the same row of the same irreducible representation of the Hamiltonian, so one needs to retain only those states for the purpose of recursion and get the same resolution as with all of them. Since the augmented space recursion retains all the properties of the real space recursion, the confinement of the recursion procedure to the irreducible portion of the Hamiltonian holds good for augmented space recursion also. The basic step in the symmetry procedure is to identify the set of nonequivalent vectors and their weights which can be achieved in augmented space by applying point point group symmetry operations to real space and configuration space independently. This reduces the rand of the augmented space Hamiltonian drastically, reducing the computer storage and, at the same time, increasing the computer speed.

4. Results and discussion

We have applied our methodology, discussed in earlier sections, to studying Cu-rich CuPd alloys and Cu-rich CuBe alloys.

4.1. Cu-rich CuPd alloys

Unlike other transition metal alloys, for example AgPd and CuNi, CuPd alloys consist of atoms belonging to different series in the periodic table and thus differing significantly in atomic number. Since the Pd 4d wavefunctions are much more extended than the Cu 3d wave-functions, making the Pd 4d bandwidth twice that of Cu, the electronic structure of CuPd alloys dilute in Pd does not show the virtual-bound state which is characteristic of CuNi and AgPd.

The electronic structure of non-isochoric Cu-rich CuPd alloys has recently attracted a considerable attention because of the controversial issue of mismatch between experimental results and theoretical analyses based on charge self-consistent KKR CPA calculations.

The disagreement between theories like KKR-based CPA [7] and experiments [6] lie in considerable suppression of the low-energy peak and in the narrowing of the Pd local density of states in the experimental data. The former effect comes from the use of same Wigner–Seitz radii for Pd and Cu atoms, leading to overscreening at the Pd site. This makes the Pd site more attractive, producing a low-energy peak. Since LMTO calculations offer one the advantage of working with different atomic sphere radii for Pd and Cu, the calculated density of states under the LMTO framework shows suppression of the low-energy peak. Secondly, the narrowing of Pd local density of states is caused by the lattice expansion around the impurity atom. The actual Cu–Pd distance is underestimated in the single-muffin-tin model. Consequently both the Cu–Pd and Pd–Pd hopping and the Pd bandwidths are overestimated. We have carried out calculations for $Cu_{95}Pd_5$ and $Cu_{75}Pd_{25}$ alloys. In figure 2(a) and (b) we present the Pd local density of states for $Cu_{75}Pd_{25}$ and $Cu_{95}Pd_5$ alloys with and without the lattice relaxation effect which shows agreement with this expectation.

In figure 3(a) and (b) we present the same for the Cu local density of states. The calculation for the Pd local density of states taking into account the lattice relaxation effect has been carried out using a single-impurity calculation of the KKR–Green function [10], LMTO CPA [11] and LAPW super-cell methods [12]. The single-impurity result has been convoluted (width 0.1 eV) by Kurdrnovský and Drchal [11] to simulate finite-concentration alloys so as to make the result comparable with that of the $Cu_{95}Pd_5$ alloy.

Bose *et al* [28] have applied the LMTO recursion method for calculating the density of states for the disordered $Cu_{75}Pd_{25}$ alloy in which configuration averaging was done by direct averaging of LDOS for 50 configurations. This, as they rightly pointed out, cannot efficiently sample all the possible environment.

If we compare our result with that of Bose *et al* result, we find that our results better reproduce the relative heights of the peaks for the Pd local density of states as obtained in CPA calculation and in the experiment of Wright *et al* [6] (shown in figure 4) where they obtained empirical results for Cu and Pd partial densities of states by taking the advantage of the copper minimum in the Pd photo-electron cross section.

For the Cu local density of states, we do not observe three sharp peaks, which are observed in CPA calculations based on the KKR method as well as the LMTO method. However this is in agreement with the experimental result of Wright *et al*. A comparative study of the characteristic quantities of component resolved density of states obtained in

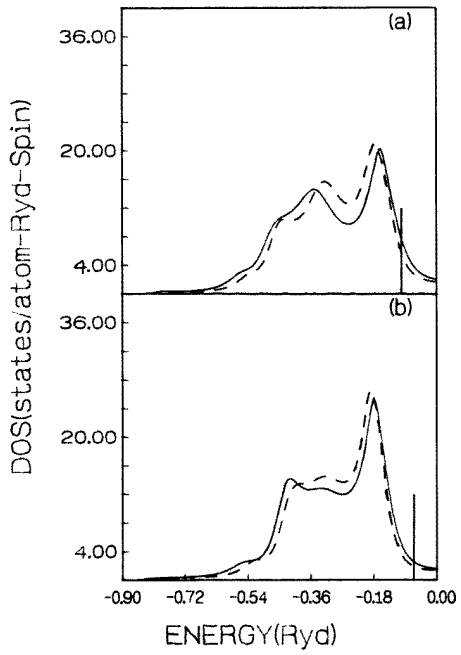

Figure 2. (a) The local densities of states on the Pd site in $Cu_{75}Pd_{25}$ alloys. The solid line represents the result without lattice relaxation and the dashed one that with the lattice relaxation effect. The vertical lines show the position of the Fermi energy. (b) The local densities of states on Pd site in $Cu_{95}Pd_5$ alloys. The solid line represents the result without lattice relaxation and the dashed one that with the lattice relaxation effect. The vertical lines show the position of the Fermi energy.

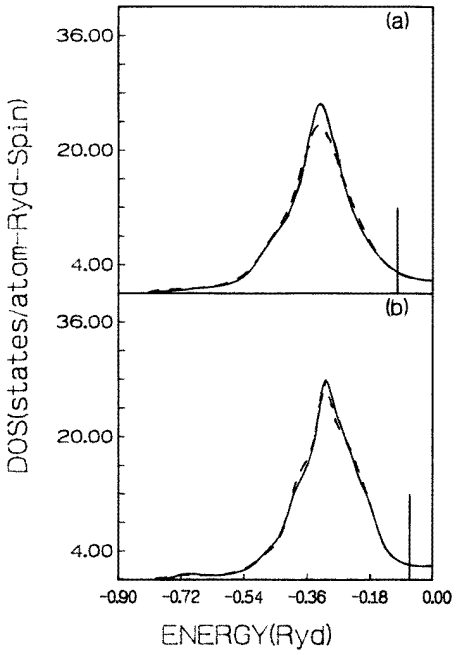

Figure 3. (a) Same as 2(a) but for local densities of states on the Cu site. (b) Same as 2(b) but for local densities of states on the Cu site.

lattice relaxed calculation of various theoretical methods has been made in tables 1 and 2 for the Pd local density of states in $Cu_{75}Pd_{25}$ and $Cu_{95}Pd_5$ alloys.

4.2. Cu-rich CuBe alloys

Cu alloyed with small amounts of Be increases the material strength of the pure metal considerably. It has been argued [29] that the slip dislocations are pinned by strong local lattice distortions (arising out of size mismatch of constituents) giving rise to high strength-to-weight ratio. Unlike CuPd where the d bands of Cu sit right in the middle of the much wider d bands of Pd, leading to a dominant d–d hybridization, in CuBe the d bands of Cu sit on the s–p hybridized bands of Be. The details of the now dominant s–d hybridization are different from the CuPd alloys.

The Be atom is smaller in radius than the Cu atom. The size mismatch between Cu and Be radii is about 10%, larger compared to that of Cu and Pd which is about 7%. Since the Be atom is smaller in radius the lattice around the Be site instead of being expanded is contracted and the use of the same hopping underestimates Be–Cu and Be–Be hopping and Be bandwidth. In figure 5 we have plotted Cu LDOS and Be LDOS for the $Cu_{95}Be_{10}$ alloy, with and without the lattice relaxation effect. While the Cu LDOS remains essentially

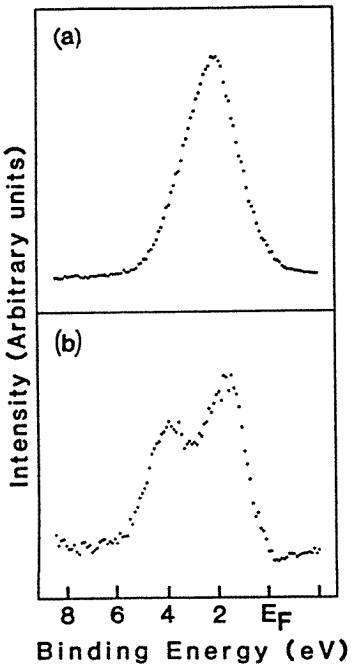

Figure 4. (a) Cu and (b) Pd LDOSs obtained from the valence-band photo-electron spectra in $Cu_{75}Pd_{25}$ of Wright *et al* [6].

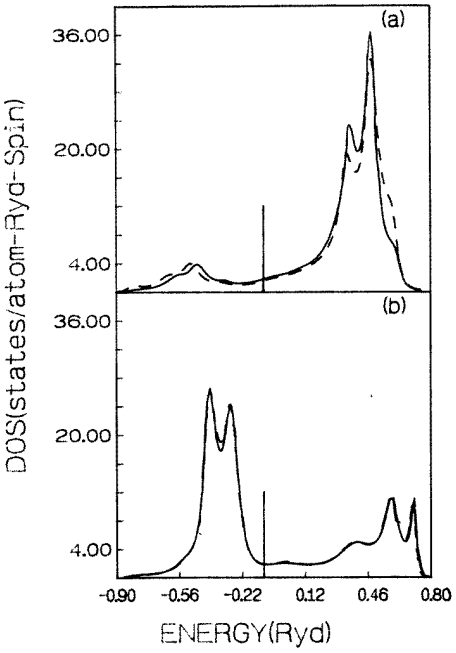

Figure 5. (a) The local densities of states on the Be site in $Cu_{90}Be_{10}$ alloys. The solid line represents the result without lattice relaxation and the dashed one that with the lattice relaxation effect. The vertical lines show the position of the Fermi energy. (b) Same as (a) but for local densities of states on the Cu site.

Table 1. Peak positions and relative peak heights of Pd local density of states (relaxed calculation) in the $Cu_{75}Pd_{25}$ alloy. Values quoted for LMTO CPA and LMTO recursion are taken from figures of [22] and the results for LAPW super-cell are taken from [24]. Peak I, peak II, peak III denote the positions of three successive peaks in the LDOS of Pd positioned from higher to lower energy. Peak positions are measured in Ryd from Fermi levels. ρ_I, ρ_{II}, ρ_{III} denote density of states at corresponding positions.

Peak position and relative peak heights	LMTO CPA	LMTO recursion	LAPW super-cell	LMTO ASR
Peak I	0.09	0.08	0.073	0.075
Peak II	0.24	0.26	0.21	0.22
Peak III	0.34	0.35	0.33	0.39
ρ_I/ρ_{II}	1.36	1.0	1.56	1.3
ρ_I/ρ_{III}	1.36	1.0	1.4	2.0

unchanged under the lattice relaxation effect with a minor effect as in CuPd alloys the Be LDOS shows a broadening effect with the centre of gravity shifted towards lower energy. In the absence of detailed experimental data and theoretical results using other methodology we are unable to give an extensive comparison. However, the principal effect of local lattice distortion in modifying local chemical bonding is also present in our results.

Table 2. Peak positions and relative peak heights of Pd local density of states (relaxed calculation) in the $Cu_{95}Pd_5$ alloy. Values quoted for LMTO CPA and KKR–Green function method are taken from figures of [8]. Peak I, peak II, peak III denote the positions of three successive peaks in the LDOS of Pd positioned from higher to lower energy. Peak positions are measured in Ryd from Fermi levels. ρ_I, ρ_{II}, ρ_{III} denote density of states at corresponding positions.

Peak position and realtive peak heights	LMTO CPA	LMTO ASR	KKR–Green function
Peak I	0.11	0.12	0.11
Peak II	0.26	0.25	0.27
PEAK III	0.35	0.34	0.38
ρ_I/ρ_{II}	1.2	1.7	1.5
ρ_I/ρ_{III}	1.2	1.7	1.5

5. Conclusions

In summary our calculation incorporating a lattice distortion effect arising out of size mismatch between constituent atoms shows a narrowing effect in the Pd LDOS for CuPd alloy and a broadening effect in the Be LDOS for CuBe alloy with the Cu LDOS practically unchanged (apart from minor changes) in either case. Our result for $Cu_{75}Pd_{25}$ are in agreement with the empirically obtained density of states, in terms of relative peak heights and peak positions. However the total energy calculation as a function of degree of lattice relaxation has to be carried out in order to obtain quantitative agreement with the prediction of EXAFS. Work in this direction is currently under way. Recently such an attempt by Zunger *et al* [12] obtained 2% expansion around the Pd site in agreement with the EXAFS result. However such a calculation as already mentioned is far more time consuming than that of the recursion method and the latter becomes increasingly powerful in presence of true positional disorder in the sense of the underlying crystal structure showing very large deviations from a regular lattice leading to glasslike network formation.

We conclude with the remark that ASR provides an formally exact way of dealing with cases where the multiplicative form of the random Hamiltonian is no longer valid. Within the terminal point approximation it is found to give a reasonable description of the lattice relaxation effect. In principle ASR can handle postionally disordered systems and can explore local environment effects.

Acknowledgments

The authors would like to acknowledge the International Centre for Theoretical Physics, Trieste for their kind invitation to the *Workshop on Condensed Matter* during which this work was completed. They would particularly acknowledge use of the ICTP computer facilities. We would like to acknowledge constant help from I Dasgupta throughout this work.

References

[1] Saha T, Dasgupta I and Mookerjee A 1994 *J. Phys.: Condens. Matter* **6** L245
[2] Mookerjee A and Prasad R 1993 *Phys. Rev.* B **48** 17 724
Dasgupta I, Saha T and Mookerjee A 1994 *Phys. Rev.* B **50** 13 267

[3] Dasgupta I 1995 *PhD Thesis* University of Calcutta
Dasgupta I and Mookerjee A 1995 submitted
[4] Kudrnovský J and Mašek 1985 *Phys. Rev.* B **31** 6424
[5] Weightman P, Wright H, Waddington S D, van der Marel D, Sawatzky G A, Diakun G P and Norman D 1987 *Phys. Rev.* B **36** 9098
[6] Wright H, Weightman P, Andrews P T, Folkerts W, Flipse C F J, Sawatzky G A, Norman D and Padmore H 1987 *Phys. Rev.* B **35** 519
[7] Winter H, Durham P J, Temmerman W M and Stocks G M 1986 *Phys. Rev.* B **33** 2370
[8] Sluiter M, de Fontaine D, Guo X Q, Podloucky R and Freeman A J 1990 *Phys. Rev.* B **42** 10 460
[9] Stefanou N, Braspenning P J, Zeller R and Dederichs P H 1987 *Phys. Rev.* B **36** 6372
[10] Stefanou N, Zeller R and Dederichs P H 1987 *Solid State Commun.* **32** 735
[11] Kudrnovský J and Drchal V 1989 *Solid State Commun.* **70** 577
[12] Lu Z W, Wei S H and Zunger A 1991 *Phys. Rev.* B **44** 3387
[13] Andersen O K and Jepsen O 1984 *Phys. Rev. Lett.* **53** 2571
[14] See articles in Andersen O K, Kumar V and Mookerjee A (ed) 1995 *Electronic Structure of Metals and Alloys* (Singapore: World Scientific)
[15] Andersen O K, Jepsen O and Glötzel D 1985 *Highlights of Condensed Matter Theory* ed F Bassani, F Fumi and M P Tosi (New York: North-Holland)
[16] Haydock R, Heine V and Kelly M J 1972 *J. Phys. C: Solid State Phys.* **5** 2845
[17] See articles in 1982 *Solid State Physics* vol 35 (New York: Academic)
[18] Mookerjee A 1973 *J. Phys. C: Solid State Phys.* **6** 1340
[19] Gray L J and Kaplan T 1976 *Phys. Rev.* B **14** 3462
[20] Mayou D, Pasturel A and Ngyuen Manh D 1986 *J. Physique* C **19** 719
Julien J P and Mayou D 1993 *J. Physique* I **3** 1861
[21] Mašek J and Kudrnovský J 1986 *Solid State Commun.* **58** 67
[22] Lucini M U and Nex C M M 1987 *J. Phys. C: Solid State Phys.* **20** 3125
[23] Andersen O K, Jepson O and Šob M 1987 *Electronic Structure and Its Applications* vol 283, ed M Yussoff (Berlin: Springer)
[24] Kudrnovský J and Drchal V 1990 *Phys. Rev.* B **41** 7515
[25] Saha T, Dasgupta I and Mookerjee A *Phys. Rev.* B submitted
[26] Chowdhury D, Gawlinski E T and Gunton J D 1987 *Comput. Phys. Commun.* **43** 329
[27] Gallagher J 1978 *PhD Thesis* University of Cambridge
[28] Bose S K, Kudrnovský J, Jepsen O and Andersen O K 1992 *Phys. Rev.* B **45** 8572
[29] Askeland D R 1989 *The Science and Engineering of Materials* (Monterey, CA: Brooks/Cole Engineering Division) p 324
[30] Lu Z W, Wei S H and Zunger A 1992 *Phys. Rev.* B **45** 10 314